Journal of Power Sources 193 (2009) 846–850

Contents lists available at ScienceDirect

Journal of Power Sources

journal homepage: www.elsevier.com/locate/jpowsour

Short communication

Electrostatic spray deposition of porous Fe_2O_3 thin films as anode material with improved electrochemical performance for lithium–ion batteries

L. Wang, H.W. Xu, P.C. Chen, D.W. Zhang, C.X. Ding, C.H. Chen*

CAS Key Laboratory of Materials for Energy Conversion, Department of Materials Science and Engineering, University of Science and Technology of China, Anhui Hefei 230026, China

ARTICLE INFO

Article history:
Received 4 January 2009
Received in revised form 9 March 2009
Accepted 31 March 2009
Available online 8 April 2009

Keywords:
Electrospray
Porous
Anode
Metal oxide
Lithium battery

ABSTRACT

Iron oxide materials are attractive anode materials for lithium–ion batteries for their high capacity and low cost compared with graphite and most of other transition metal oxides. Porous carbon-free α-Fe_2O_3 films with two types of pore size distribution were prepared by electrostatic spray deposition, and they were characterized by X-ray diffraction, scanning electron microscopy and X-ray absorption near-edge spectroscopy. The 200 °C-deposited thin film exhibits a high reversible capacity of up to 1080 mAh g^{-1}, while the initial capacity loss is at a remarkable low level (19.8%). Besides, the energy efficiency and energy specific average potential (E_{av}) of the Fe_2O_3 films during charge/discharge process were also investigated. The results indicate that the porous α-Fe_2O_3 films have significantly higher energy density than $Li_4Ti_5O_{12}$ while it has a similar E_{av} of about 1.5 V. Due to the porous structure that can buffer the volume changes during lithium intercalation/de-intercalation, the films exhibit stable cycling performance. As a potential anode material for high performance lithium–ion batteries that can be applied on electric vehicle and energy storage, rate capability and electrochemical performance under high-low temperatures were also investigated.

1. Introduction

Lithium–ion batteries (LIB) are currently widely used as power sources for various electronic devices including laptops, cellular phones and camcorders. For the portable consideration, there is a demand to improve either gravimetric or volumetric energy density of commercial lithium–ion batteries. Graphite is the-state-of-the-art anode material in commercial lithium–ion batteries, but its limited capacity (theoretically 372 mAh g^{-1}) provides a motivation to develop new anode materials. As potential alternatives for graphite, transition metal oxides MO_x (M=Fe, Co, Ni, etc.) attract lots of attention in recent years [1–9]. They usually have a capacity of up to over 1000 mAh g^{-1}, which is much higher than the carbonaceous anode materials. Nevertheless, they work in a mechanism of the so-called conversion reaction, i.e. $MO_x + 2xLi \rightarrow M + xLi_2O$, that is different from the intercalation/de-intercalation mechanism. Usually, a large volume expansion always occurs during the charge–discharge process due to the generation of Li_2O so that the active materials may break off from the current collector, leading to capacity fading very quickly [10]. Thus, it becomes important to overcome this obstacle and develop strategies to improve the cycling capability of transition metal oxides. During the last decade, lots of efforts have been made to pursue improved electrochemical properties of metal oxides [11–14].

In our previous studies, we have reported a series of porous metal oxides films prepared by electrostatic spray deposition (ESD), such as CoO, Cu_2O, NiO, and found that porous structures can effectively buffer the volume expansion while lithium inserting the electrode [15–17]. Here we report the synthesis and electrochemical performance of novel carbon-free α-Fe_2O_3 films with a porous structure prepared by ESD. Considering the fact that the working potentials of metal oxide anodes are usually markedly higher than lithiated carbon, we propose a new parameter, i.e. energy specific average potential (E_{av}), to quantitatively evaluate this factor. We have thus optimized the deposition temperature to obtain a α-Fe_2O_3 film with a high reversible capacity, long cycle life and remarkable rate capability. Except for these basic electrochemical properties, their energy efficiency and electrochemical behaviors under high/low temperatures are also investigated, aiming at the possibility of applications in EV/HEV and energy storage.

2. Experimental

Thin films were prepared through electrostatic spray deposition (ESD) technique. 0.5 mmol $Fe(NO_3)_3{\cdot}9H_2O$ was dissolved into a mixture of 80 mL 1,2-propylene glycol and 20 mL ethanol to obtain a precursor solution for ESD after a continuous stirring for 1 h. During the film deposition, a 15 kV direct current voltage was applied

* Corresponding author. Tel.: +86 551 3606971; fax: +86 551 3601592.
E-mail address: cchchen@ustc.edu.cn (C.H. Chen).

0378-7753/$ – see front matter © 2009 Elsevier B.V. All rights reserved.
doi:10.1016/j.jpowsour.2009.03.063

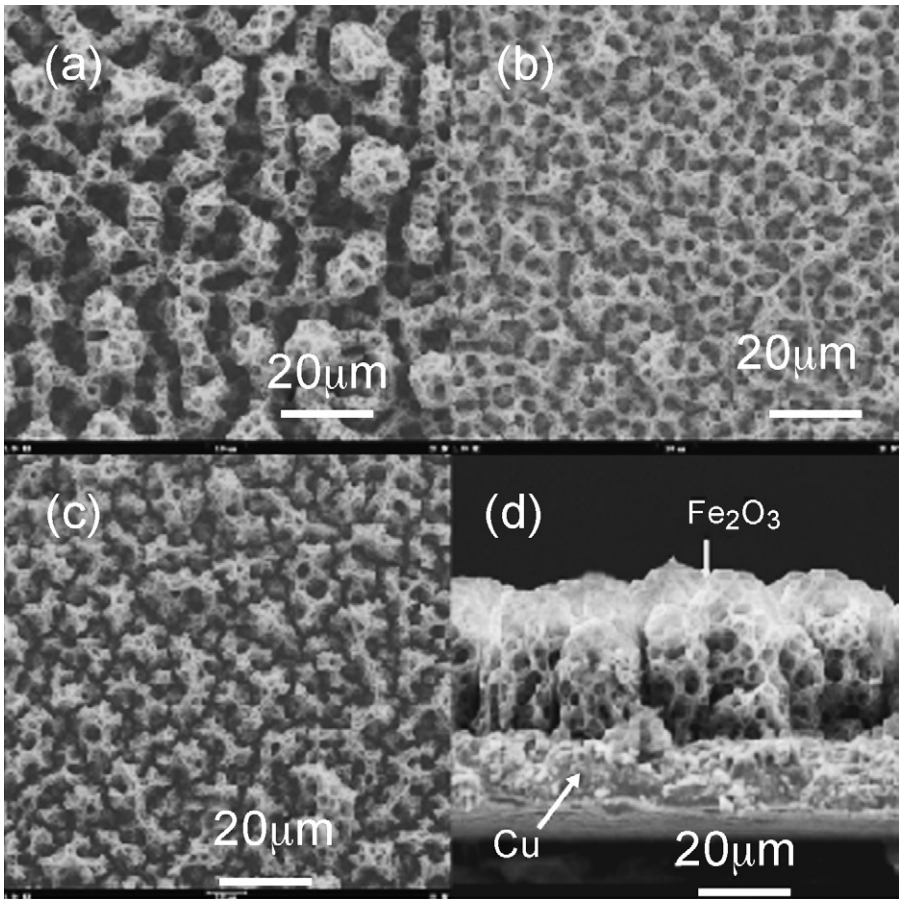

Fig. 1. SEM images of thin films deposited at 170 °C (a), 200 °C (b) and 240 °C (c).

between the metallic nozzle and substrate, and the flow rate was controlled at 40 μL min^{-1} by a syringe pump. The substrate was heated at different temperatures of 170, 200, 230 °C, respectively. All the thin films are controlled with the same area of 1.13 cm^2. They were weighed in a balance and the weight of the films was usually about 1.5 mg. The morphology of the as-deposited films was studied under a scanning electron microscope (Hitch X650). Their composition and crystal structure of thin films were characterized by X-ray diffraction (Philips X'Pert Pro Super, Cu Kα radiation).

The electrochemical properties of the films were characterized using 2032 coin cells. The films were directly used as working electrode without any treatment, and a lithium metal sheet was used as the counter electrode, while the electrolyte was 1 M $LiPF_6$ in ethylene carbonate/dimethyl carbonate (1:1 v/v). The cells were assembled in an argon-filled glove box (MBRAUN LABMASTER 130) with moisture and oxygen levels less than 1 ppm. The cells were cycled in the voltage range between 3.0 V and 0 V on a multichannel battery cycler (NEWWAEE BTS-610). After 20 cycles, the cell was disassembled in the glove box, and the thin film electrode was washed with dimethyl carbonate for ex situ SEM analysis. To measure the cycling performance at different temperatures, the cells were also cycled at 5, 10, 25, 55 °C, respectively, in a high-low temperature chamber.

3. Results and discussions

Fig. 1 shows the surface morphology of the as-deposited films deposited at different temperatures. All three films exhibit a reticular three dimensionally porous structure which is similar to our early reported results on other ESD-derived materials [16]. Interestingly, different from the sponge-like structure, the films contain two types of micropores with different pore sizes, the larger one ranging from 5 to 10 μm, and the smaller one about 1 μm on the wall of the cross-linking structure. Obviously, the porous structure is related to the solvent evaporation and decomposition of inorganic salts. When the substrate temperature is 170 °C, that is below the boiling point (183 °C) of 1,2-propylene glycol, the droplets have enough time to spread on the heated substrate before the solvent evaporates completely (Fig. 1a). This slow evaporation process leads to a loose structure and large pore sizes of the deposited films. When the substrate temperature is 200 °C, the pore size becomes smaller and the film seems to be denser (Fig. 1b). As the substrate temperature further increases to 230 °C, the film is somewhat similar to the 200 °C-deposited ones but with the appearance of some cracks (Fig. 1b and c). In addition, the thickness of the film can be clearly seen as about 30 μm from the cross section image of 200 °C-deposited thin film (Fig. 1d).

The composition and crystalline structure of the as-deposited films were also studied by X-ray diffraction (Fig. 2a). For the purpose of reducing the disturbance signals of the substrate, a stainless foil is used here as substrate because it has less number of diffraction peaks compared with copper foil. Obviously, the crystallinity of the films deposited at higher temperature is better. For the 200 °C-deposited film, only a weak broad diffraction peak near 35° is observed except for those of the substrate. However, for the 230 °C-deposited film, some strong peaks are visible near 33.0°, 35.6°, 49.3°, 53.9°, 62.3° and 63.9°, which correspond to the (1 0 4), (1 1 0), (0 2 4), (1 1 6), (2 1 4), and (3 0 0) diffraction peaks of hematite (α-Fe_2O_3, JC PDF 86-0550), respectively. Hence we conclude that when the substrate temperature is 200 °C, the Fe_2O_3 particles are poorly

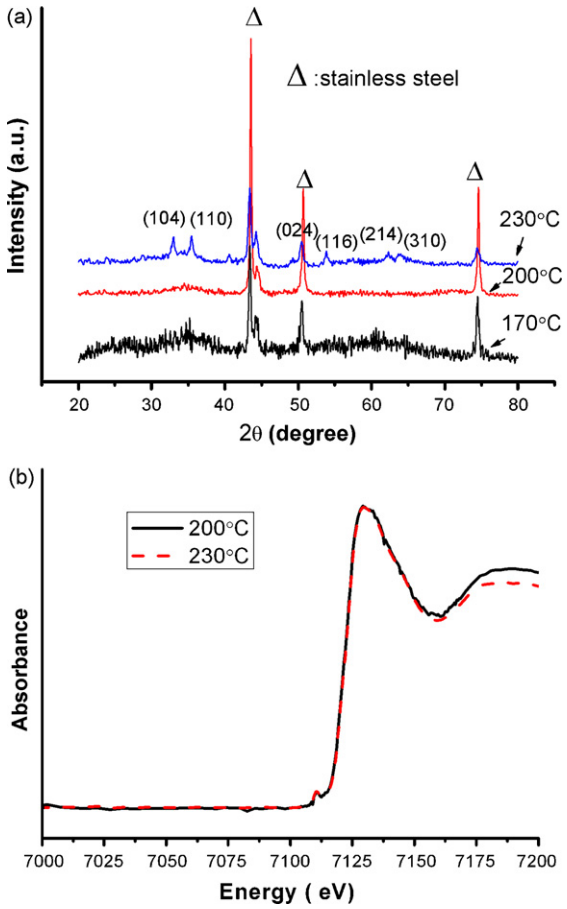

Fig. 2. XRD patterns of the as-deposited films (a) and XANES patterns of 200 °C- and 230 °C-deposited films (b).

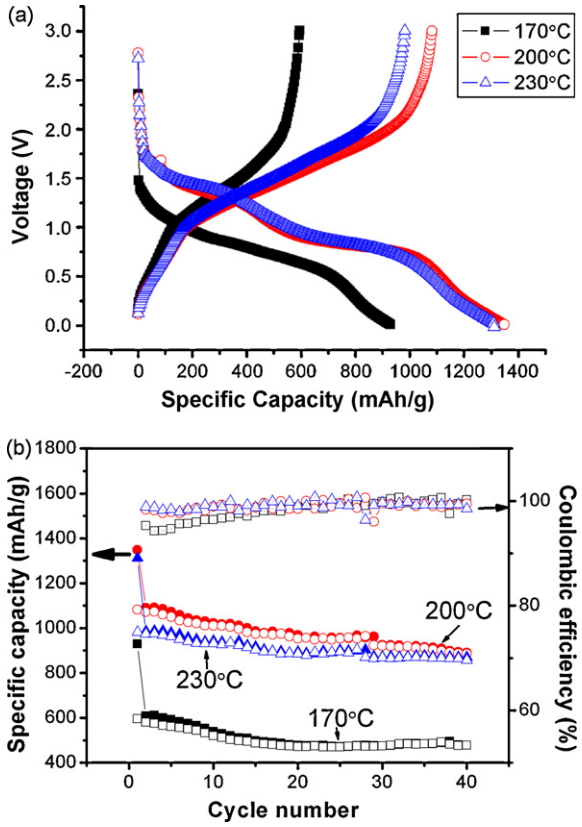

Fig. 3. (a) Voltage profiles of the Fe_2O_3 films in the first discharge–charge cycle; (b) Specific capacity and Coulombic efficiency vs. cycle numbers for the Fe_2O_3 thin films deposited at different temperatures: 170 °C (square), 200 °C (cycle) and 230 °C (triangle). (c) Ex situ SEM image of 200 °C-deposited film cycled for 20 cycles. All of the cells were cycled between 0 and 3 V at a current density of 270 mA g^{-1}.

crystallized compared with that deposited at 230 °C. From their X-ray absorption near edge spectra (XANES), it is found that both 200 °C- and 230 °C-deposited films have nearly the same absorption spectra, meaning the valence of iron is the same (+3) in these two samples.

Although there is no conducting additive such as carbon in above Fe_2O_3 films, they are still electrochemically active because Fe_2O_3 itself is a semiconducting oxide that has sufficient electronic conductivity. Fig. 3a shows the first-cycle voltage profiles of the Fe_2O_3 films measured using Fe_2O_3/Li half cells. They are typical charge–discharge curves for a transition metal oxide anode material. For example, for the 200 °C-deposited film, at the beginning of discharge, the voltage decreases quickly to approximately 1.75 V, whereupon a plateau appears until a specific capacity of 145 mAh g^{-1} (corresponding to 0.9 mol of Li per mole of Fe_2O_3). This profile is rather close to the result of a nanometer-sized Fe_2O_3 powder observed by Tarascon et al. [18]. Because of the absence of this plateau in micro-sized Fe_2O_3, these ESD derived Fe_2O_3 films should be nano-size scaled. When fully discharged to 0 V, a high capacity of 1350 mAh g^{-1} is achieved, equal to 8.0 mol of Li per mole of Fe_2O_3. Such a high capacity suggests that about 2 mol of Li (corresponding to 335 mAh g^{-1}) has been consumed to form solid electrolyte interface (SEI) film and some reversible surface layer in addition to complete reduction of iron from +3 to 0 [22,23]. In literature, various values of the first discharge capacity of Fe_2O_3, have been reported, which seems to indicate that the film morphology plays a significant role in the discharge process [19–21].

On the other hand, the first charge capacity of the films deposited at 170 °C, 200 °C and 230 °C is 595 mAh g^{-1}, 1080 mAh g^{-1} and 982 mAh g^{-1}, respectively. Therefore, the first cycle energy density for the optimal 200 °C-deposited film can be calculated as 460 mAh cm^{-3} for the charge and 570 mAh cm^{-3} for the discharge. Assuming that the surface layer from electrolyte decomposition is completely reversible, the charge capacity of 200 °C-deposited film would reach to 1005 mAh g^{-1} when all of the Fe^0 are oxidized to Fe^{2+}. Actually the SEI film is always passivated and irreversible, so we can conclude that part of Fe can be oxidized back to Fe^{3+}. This is consistent with Tarascon et al.'s result [18]. Meanwhile, the initial capacity loss of the films deposited at these three temperatures is 35.9%, 19.8% and 25.2%, respectively. Thus, the 200 °C-deposited film not only exhibits the highest capacity, but also has the lowest initial capacity loss of 19.8%. Considering that the usually large initial capacity loss (>30%) is one of the obstacles of commercialization of metal oxides, our result seems to give a way to solve this problem.

Another obstacle of metal oxide anodes is with their large voltage hysteresis between charge and discharge processes. Hence, it is necessary to study the energy efficiency of metal oxides. Table 1 shows the second cycle energy efficiency of the films deposited at different temperatures. The energy efficiency and the energy specific average potential (E_{av}) are calculated by integrating the voltage profiles with regard to the specific capacity. Different from graphite which usually has an energy efficiency of over 90%, α-Fe_2O_3 exhibits a low energy efficiency of around 60%. Among the films deposited at 170, 200 and 230 °C, the 200 °C-deposited film exhibits the highest energy efficiency of 65.8%. Though this efficiency is still much lower than that of graphite, it is still higher than those of CoO, Cu_2O, SnO_2 and so on because their energy efficiencies are usually between 55% and 60%.

Table 1
Energy efficiency and energy specific average potential of the as-deposited Fe_2O_3 films.

Deposition temperature	Energy density of 1st charge (Wh kg^{-1})	Energy density of 2nd discharge (Wh kg^{-1})	Energy efficiency	E_{av} of 1st charge (V)
170 °C	800	468	58.6%	1.35
200 °C	1640	1080	65.8%	1.51
230 °C	1460	944	64.7%	1.48

For a material to be considered as an anode material for high power lithium–ion batteries, it is necessary to evaluate its working potential versus Li. We may define a term, energy specific average potential (E_{av}) for this purpose, which may be calculated by the integrated energy divided by the capacity during a charge or discharge process of a half-cell. This energy specific average potential can effectively represent the power capability of a cell that can be achieved if such an electrode is used in a battery. Our results indicate that the energy specific average potential E_{av} of the 200 °C-deposited film is 1.51 V (Table 1), which is rather close to the charge/discharge potential of $Li_4Ti_5O_{12}$. Therefore, this porous α-Fe_2O_3 film is a possible candidate anode material for high power LIB.

Fig. 3b shows the cycling performance of the films deposited at three temperatures. Compared with the bulk α-Fe_2O_3 [18,21], all of these films exhibit relatively better capacity retention. The 200 °C-deposited film has the highest discharge capacity in the 2nd cycle (1090 mAh g^{-1}), and it still retains 896 mAh g^{-1} after 40 cycles. Thus, there is about a capacity loss of 0.45% per cycle. For the 230 °C-deposited film, the discharge capacity of the 2nd cycle decreases to 990 mAh g^{-1}, but its cycling performance seems even better than the 200 °C-deposited one. After 40 cycles, a capacity of 874 mAh g^{-1} is delivered, corresponding to 82% of the 2nd cycle, and 0.3% capacity drop per cycle. All of these good cycling performances should be related to the porous structure of the films, which can buffer the volume expansion during cell cycling so that the active materials will not fall off the current collector. Ex situ SEM analysis is conducted to investigate the morphology change during charge–discharge cycles. Fig. 3c exhibits the SEM image of a 200 °C-deposited thin film that has been cycled for 20 cycles. Generally speaking, the porous structure seems in good condition and there is even no visible crackle on the surface. Therefore, we can conclude that the cycling performance of Fe_2O_3 electrode is enhanced by the porous structure because it can effectively buffer the volume expansion and shrinkage during cell cycling.

For the purpose of applications of LIB to hybrid energy vehicle (HEV), good rate capability is necessary for both of the cathode and anode materials. The rate capability test has been conducted on the 200 °C-deposited film. Fig. 4a shows the discharge capacity under different current density range from 0.5 C to 5 C (1 C is equivalent to 1080 mA g^{-1}). Due to the particular porous structure, the film exhibits excellent rate capability. At current density of 0.5 C, the discharge capacity is 930 mAh g^{-1}, which is almost the same as that at 0.2 C. With the current density further increased up to 1 C, the capacity drops to 790 mAh g^{-1}, corresponding to 58.6% of the capacity at 0.2 C. Finally, when the cell is cycled at a high current density of 5 C, it can deliver a capacity of 508 mAh g^{-1}, which is even higher than the theoretical capacity of graphite (372 mAh g^{-1}). There are two possible reasons that may account for this good rate capability. Firstly, the contact area between Fe_2O_3 particles and electrolyte is large because of the porous structure. Secondly, the films are actually composed of nanoparticles as confirmed in our previous study [16], hence the rate performance can benefit from the much reduced diffusion distance. This result may be meaningful to the development of EV and HEV, both of which require high reversible capacity under a rapid charging–discharging condition.

On the other hand, as a power source of EV or HEV, the batteries must be stable in cruel environment such as a wide temperature range from cold winter to hot summer. Thus, the cell made of the 200 °C-deposited film has been tested from a high temperature of 55 °C down to a low temperature of 5 °C (Fig. 4b). The reversible capacity is as high as 1350 mAh g^{-1} at 55 °C, which is much higher than at room temperature. It is also higher than the theoretical capacity of α-Fe_2O_3 based on the conversion reaction. A similar phenomenon of Co based oxides has been reported by Tarascon's group [22]. At the elevated temperature of 75 °C, they measured a discharge capacity up to 1700 mAh g^{-1}. They concluded that the extra capacity comes from the electrolyte decomposition, forming a polymer/gel-like film which is reversible during charge–discharge cycling. Maier's group employed an interfacial lithium storage model to explain where the extra capacity comes from [23]. Therefore, in our case, when the temperature rises up, it becomes easier to form more gel-like film or to store more lithium in the interface between metal and Li_xO. Contrarily, when the temperature falls down, the capacity contribution of this gel-like film or interfacial lithium storage decreases. When discharged at 15 °C, the film shows an obvious capacity drop and its reversible capacity is 840 mAh g^{-1}.

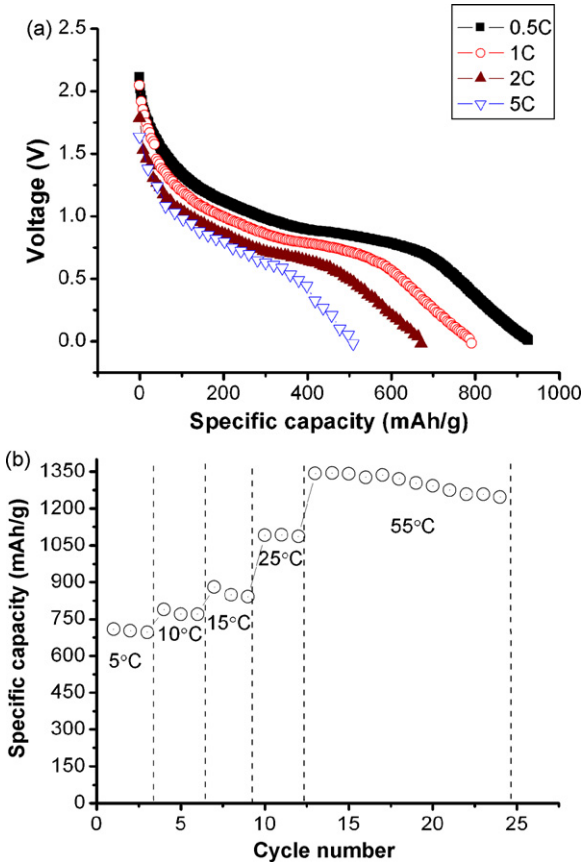

Fig. 4. (a) Discharge voltage profiles of the 200 °C-deposited film at different current densities. The cell was cycled at 0.25 C for three times before the rate capability test. (b) Electrochemical performance of the 200 °C-deposited film at different temperatures.

At 10 °C and 5 °C, the capacity is 770 mAh g^{-1} and 690 mAh g^{-1}, respectively. Compared with the traditional anode material such as graphite whose theoretical capacity is only 372 mAh g^{-1}, these results are quite attractive. It means that we may develop a battery which is smaller, lighter than the current commercial ones, but it can work in cruel environments either hot or cold.

4. Conclusions

In this study, porous carbon-free α-Fe_2O_3 films have been prepared at different temperatures by electrostatic spray deposition, and the 200 °C-deposited film exhibits excellent electrochemical behaviors. It has both high reversible capacity (1080 mAh g^{-1}) and good cycling performance. Most importantly, it shows the highest energy efficiency with the lowest initial capacity loss ever reported for Fe_2O_3 anode. Aiming at the anode material for high-power lithium–ion batteries, the 200 °C-deposited α-Fe_2O_3 film has an acceptable energy specific average potential around 1.5 V, which is similar to $Li_4Ti_5O_{12}$. Considering its good rate capability, excellent electrochemical behaviors at high and low temperatures and its low cost, such an optimized ESD prepared film provides a candidate of anode material for lithium–ion batteries in the applications of HEVs.

Acknowledgement

This study was supported by Education Department of Anhui Province (Grant no. KJ2009A142).

References

[1] P. Poizot, S. Laruelle, S. Grugeon, L. Dupont, J.M. Tarascon, Nature 407 (2000) 496–499.
[2] A.S. Arico, P.G. Bruce, B. Scrosati, J.M. Tarason, W.V. Schalkwijk, Nat. Mater. 4 (2005) 366–377.
[3] J. Chen, L.N. Xu, W.Y. Li, X.L. Gou, Adv. Mater. 17 (2005) 582–586.
[4] K.T. Nam, D.W. Kim, P.J. Yoo, C.Y. Chiang, N. Meethong, P.T. Hammond, Y.M. Chiang, A.M. Belcher, Science 312 (2006) 885–888.
[5] W.Y. Li, L.N. Xu, J. Chen, Adv. Funct. Mater. 15 (2005) 851–857.
[6] X.H. Huang, J.P. Tu, C.Q. Zhang, J.Y. Xiang, Electrochem. Commun. 9 (2007) 1184–1187.
[7] P.L. Taberna, S. Mitra, P. Poizot, P. Simon, J.M. Tarascon, Nat. Mater. 5 (2006) 567.
[8] C.Z. Wu, P. Yin, X. Zhu, C.Z. Ouyang, Y. Xie, J. Phys. Chem. B 110 (2006) 17806–17812.
[9] L. Tabernal, S. Mitra, P. Poizot, P. Simon, J.M. Tarascon, Nat. Mater. 5 (2006) 567–573.
[10] J. Hu, H. Li, X.J. Huang, Electrochem. Solid State Lett. 8 (2005) A66–A69.
[11] G. Binotto, D. Larcher, A.S. Prakash, R. Herrera Urbina, M.S. Hegde, J.M. Tarascon, Chem. Mater. 19 (2007) 3032–3040.
[12] X.H. Huang, J.P. Tu, C.Q. Zhang, X.T. Chen, Y.F. Yuan, H.M. Wu, Elechtrochim. Acta 52 (2007) 4177–4181.
[13] L.J. Zhi, Y.S. Hu, B.E. Hamaoui, X. Wang, I. Lieberwirth, U. Kolb, J. Maier, K. Mullen, Adv. Mater. 20 (2008) 1727–1731.
[14] Y.G. Li, B. Tan, Y.Y. Wu, Nano Lett. 8 (2008) 265–270.
[15] Y. Yu, C.H. Chen, J.L. Shui, S. Xie, Angew. Chem. Int. Ed. 44 (2005) 7085–7089.
[16] Y. Yu, Y. Shi, C.H. Chen, Nanotech 18 (2007) 055706.
[17] Y. Yu, C.H. Chen, Y. Shi, Adv. Mater. 19 (2007) 993–997.
[18] D. Larcher, D. Bonnin, R. Cortes, I. Rivals, L. Personnaz, J.-M. Tarascon, J. Electrochem. Soc. 150 (2003) A1643–A1650.
[19] M.V. Reddy, T. Yu, C.H. Sow, Z.X. Shen, C.T. Lim, G.V. Subba Rao, B.V.R. Chowdari, Adv. Funct. Mater. 17 (2007) 2792–2799.
[20] Y. NuLi, R. Zeng, P. Zhang, Z.P. Guo, H.K. Liu, J. Power Sources 184 (2008) 456–461.
[21] F. Jiao, J.L. Bao, P.G. Bruce, Electrochem. Solid State Lett. 10 (2007) A264–A266.
[22] S. Grugeon, S. Laruelle, L. Dupont, J.M. Tarascon, Solid State Sci. 5 (2003) 895–904.
[23] J. Jamnik, J. Maier, Phys. Chem. Chem. Phys. 5 (2003) 5215–5220.